C_α−H Bond-Stretching Frequency in Alcohols as a Probe of Hydrogen-Bonding Strength: A Combined Vibrational Spectroscopic and Theoretical Study of *n*-[1-D]Propanol

S. Jarmelo,[†] N. Maiti,[‡] V. Anderson,[‡] P. R. Carey,[‡] and R. Fausto*[,†]

Department of Chemistry, University of Coimbra, 3004-535 Coimbra, Portugal, and Department of Biochemistry, Case Western Reserve University, 10900 Euclid Avenue, Cleveland Ohio 44106-4935

Received: July 26, 2004; In Final Form: December 27, 2004

The sensitivity of the $\nu_{C_\alpha-H/D}$ vibrational stretching frequency to hydrogen bonding in alcohols is examined by infrared and Raman spectroscopy, supported by DFT(B3LYP)/6-311++G(d,p) calculations. The model compound studied is (*R*,*S*)-*n*-[1-D]propanol. It is shown that the $\nu_{C_\alpha-H/D}$ mode can be successfully correlated with the hydrogen-bond strength in a given solvent, provided the O−H group involved in the hydrogen bond is not acting simultaneously as a hydrogen-bond donor and acceptor. In addition, a detailed analysis of the spectroscopic features observed in both the ν_{O-H} and $\nu_{C_\alpha-H/D}$ spectral regions of the spectra of *n*-propanol and (*R*,*S*)-*n*-[1-D]propanol, in a series of different experimental conditions, which include the matrix-isolated compound (in argon matrix), pure liquid and low-temperature glassy states, and solution in different solvents, is undertaken. This permits the contribution of the different conformers of the studied compounds to be assigned to the bands observed in the ν_{O-H} and ν_{C-H} spectral regions.

Introduction

Hydrogen bonding is one of the most important intermolecular forces between substrate and enzyme active-site residues. The presence of a single hydrogen bond at an enzyme active site can be crucial to catalysis.[1] Their presence have been confirmed in almost every crystal structure of enzyme·substrate complexes determined so far.

While the existence and importance of these hydrogen bonds is beyond doubt, methods to determine the energetic contribution of individual hydrogen bonds to binding and catalysis are not readily available. Sub-angström *X-ray crystallography* is becoming progressively accessible, providing opportunities to study protein structures at much higher resolutions than were previously attained and enabling direct measurement of hydrogen-bond distances.[2] A strong correlation exists between hydrogen-bond distances and energies. However, small differences of 0.1 Å correspond to large differences in energy, making the uncertainty in the crystallographically determined hydrogen-bond distances still a critical factor in the estimation of hydrogen-bond strengths by this method. On the other hand, it can only be used to study crystalline samples. *Site-directed mutagenesis* has revealed that removing an hydrogen-bond donor or acceptor can reduce the catalytic efficiency of an enzyme by a factor as large as 10^5.[3] However, possible structural changes make this method equivocal. *NMR spectroscopic* detection of highly deshielded protons has been suggested to enable identification of strong hydrogen bonds at enzyme active sites,[4] but these results still remain controversial. The NMR approach is also limited to protons that exchange slowly with the solvent.

Determination of hydrogen-bond strengths by *vibrational spectroscopic* methods usually relies on measurement of the stretching frequency of the donor group in anhydrous solvents.[5] Correlations of the O−H stretching frequency with the hydrogen-bond strength have been developed.[6,7,8,9] However, this approach cannot be used successfully for most of the biochemically relevant systems, where the background absorption (or scattering) from the solvent, water, obscures all of the relevant stretching frequencies of the desired enzyme·substrate complex. Deuterium substitution of the hydroxyl proton does not help because of the rapid exchange with the solvent, while ^{18}O labeling does not sufficiently perturb the frequency to differentiate the $^{18}O-H$ stretching from the intense water bands. Therefore, a novel approach has been developed in our laboratories to determine the strength of individual hydrogen bonds in enzyme active sites, which is based on the premise that this property is reflected in the $C_\alpha-H$ bond of the $H-C_\alpha-O-H$ functional group in primary and secondary alcohols acting as hydrogen-bond donors.[10,11] This idea is an extension of the observation that the $C_\alpha-H$ stretching frequency is a function of the torsion angle about the $C_\alpha-O$ bond.[5a,b] In primary and secondary alcohols, either a lone pair of electrons or the σ-bonding electrons of the O−H bond will be anti to the $C_\alpha-H$ bond. If the O−H bond is anti to the $C_\alpha-H$ bond, the bonding electrons exhibit greater delocalization as the proton is progressively removed by hydrogen bonding. This delocalization results in a larger overlap with the σ^* antibonding orbital of the $C_\alpha-H$ bond and, consequently, decreases the $C_\alpha-H$ bond order and its associated vibrational stretching frequency.

Single-deuterium substitution in the α-carbon atom strongly increases the capabilities of this new approach, because the $C_\alpha-D$ stretching appears in a spectral region (2250−2000 cm^{-1}) where contributions from other vibrations are minimal. Moreover, the unusual frequency of $\nu_{C_\alpha-D}$ moiety also minimizes the coupling with other vibrational modes and, to a good approximation, may be interpreted as a simple group frequency.

In this work, a suitable simple model primary alcohol (*n*-[1-D]propanol) is used to further investigate the effects of hydrogen bonding on the $C_\alpha-D$ stretching vibration and establish useful correlations between the hydrogen-bond strength and vibrational/structural data.

* To whom correspondence should be addressed. E-mail: rfausto@ci.uc.pt.
[†] University of Coimbra.
[‡] Case Western Reserve University.

10.1021/jp046683c CCC: $30.25
Published on Web 02/16/2005

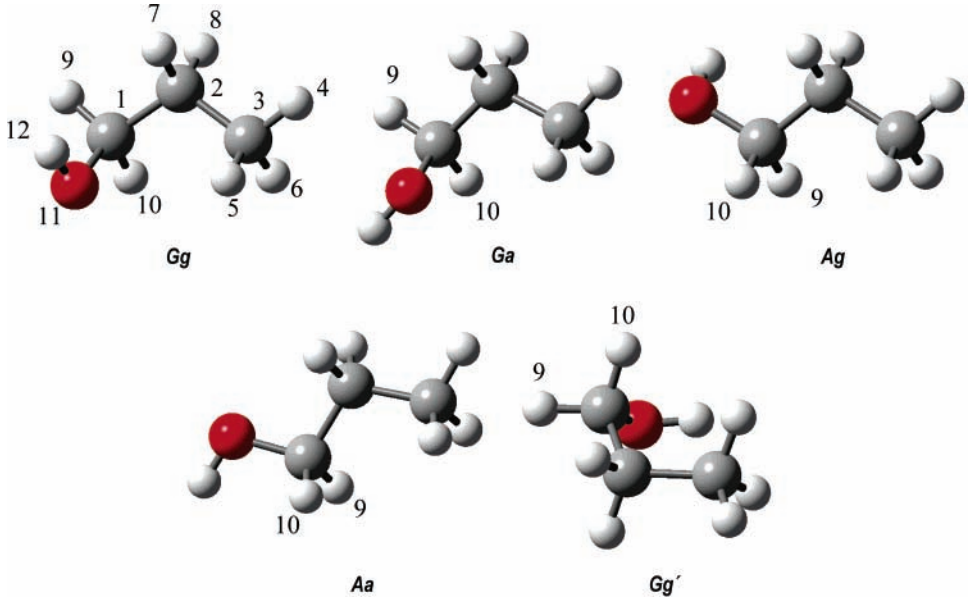

Figure 1. Conformers of *n*-propanol and atom numbering. In the nonisotopically substituted molecule, G′g′, G′a, Ag′, and G′g are mirror images of Gg, Ga, Ag, and Gg′, respectively.

Experimental and Computational Methods

(*R*,*S*)-*n*-[1-D]Propanol was obtained from ICON Stable Isotopes, with a deuterium content larger than 98%. All of the remaining substances used in this study, including solvents, were obtained from Aldrich, at spectroscopic grade.

Raman Spectroscopy. Raman spectra were obtained using 647.1 nm laser excitation from an Innova 400 krypton laser system (Coherent, Inc.), a back-illuminated charge-coupled device (CCD) detector (model 1024EHRB/1, Princeton Instruments, Inc.) operating at 183 K, and a Holospec f/1.4 axial transmission spectrometer (Kaiser Optical Systems, Inc.) employed as a single monochromator, as described in ref 12. The Raman spectra of (*R*,*S*)-*n*-[1-D]propanol were acquired for the neat liquid and solution (10 mM) in chloroform, toluene, and carbon tetrachloride. Tertiary amine hydrogen-bond acceptors were used: triethylamine, *N*,*N*-diisopropylethylamine, *N*-methylmorpholine, and *N*,*N*-dimethylaniline. The concentrations used in the mixed (*R*,*S*)-*n*-[1-D]propanol/hydrogen-bond acceptor solutions (in $CHCl_3$) were 10 mM (*R*,*S*)-*n*-[1-D]propanol and 500 mM amine acceptor. The samples (60 μL) were held in a 2 × 2 mm quartz cuvette under the 90° excitation/collection geometry, and the Raman spectra were collected using a laser power of ≅150 mW and CCD exposure times of 1 min. For each spectrum, generally 10 exposures were acquired. The solvent spectrum was subtracted, and the baseline correction was made by multipoint selection. Wavenumber calibration was performed by recording the Raman spectra of the 1:1 mixture of cyclohexanone and acetone-D_6, providing band positions to within ±1 cm^{-1} for sharp bands. Data analysis was carried out using GRAMS/32 and ORIGIN 7.0.[13]

Infrared Spectroscopy. Low-temperature spectra of the compound as a solid film and in argon (Air Liquid, argon, 99.9999%) matrix were obtained in the range of 4000−400 cm^{-1} using a Mattson (Infinity 60AR Series) Fourier transform infrared spectrometer equipped with a deuterated triglycine sulfate (DTGS) detector and Ge/KBr beam splitter. Data collection was performed with 0.5 cm^{-1} spectral resolution. All experiments were done based on an APD Cryogenics close-cycle helium refrigeration system with a DE-202A expander. Further details of the experimental set up can be found in ref 14.

Theoretical (DFT) Calculations. All theoretical calculations were performed with Gaussian 98.[15] The standard 6-311++G-(d,p) and 6-31+G(d) basis sets[16,17,18] and the three-parameter density functional, B3LYP, which includes Becke's gradient exchange correction[19] and the Lee, Yang, and Parr correlation functional,[20] were selected for the calculations, providing a good compromise between the expected quality of the results and computational resources. The calculated frequencies were scaled down by an appropriate factor (0.978),[21,22,23] except for the ν_{O-H} stretching region (whereas the scale factor used was 0.954, chosen to fit the experimental data), to correct them for the effects of basis set limitations, anharmonicity, and correlation, and used to assist the analysis of the experimental spectra. Solvent effects were taken into account in the calculations [B3LYP/6-311++G(d,p)] by using the polarized continuum model (PCM),[24] with the geometries of the different conformers reoptimized for each solvent considered.

Results and Discussion

n-Propanol has two internal rotation axes leading to conformational isomerism (rotation of the CH_3 group does not give rise to different conformers). For this molecule, there are five nonequivalent putative conformers, denoted in this paper by Gg, Gg′, Ga, Ag, and Aa (Figure 1). In the notation used here, the capital letter refers to the conformation of the CCCO axis and the lowercase letter refers to the conformation of the CCOH axis; G and g = gauche (60°) and A and a = anti (180°); the prime indicates a negative value for the corresponding dihedral angle. Conformers G′g′, G′g, G′a, and Ag′ are spectroscopically and energetically equivalent to their mirror images Gg, Gg′, Ga, and Ag, respectively; thus all of these conformers have statistical weights equal to 2.

Despite its moderate size, *n*-propanol has not been the subject of many studies. A normal coordinates study on this compound was reported in the late sixties.[25] In that study, the authors used a modified Urey−Bradley force field to predict the frequencies of the light and deuterated (OD) isotopologues and perform an assignment of the previously registered infrared and Raman spectra for the compounds in the vapor phase.[26,27] In those calculations, an approximate molecular geometry was used and the spectra were interpreted based on conformational isomerism

TABLE 1: Relevant Dihedrals, Electronic Energy (E), Zero-Point Energy (ZPE), Relative Energy (ΔE) to the Most Stable Form (with and without ZPE correction) and Dipole Moment (μ) for the Different Conformers of *n*-Propanol, Calculated at the DFT/B3LYP/6-311++G(d,p) Level of Theory

conformer	$CCCO_{al.}$ (deg)	$CCOH_{al.}$ (deg)	E (kJ mol^{-1})	ZPE (kJ mol^{-1})	ΔE_{ZPE} (kJ mol^{-1})	ΔE (kJ mol^{-1})	μ (Debye)
Aa	180.00	−180.00	−510 448.07	277.41	0	0.14	1.653
Ga/G′a	63.68	−177.71	−510 448.15	277.54	0.05	0.07	1.776
Gg/G′g′	61.47	64.43	−510 447.80	277.92	0.78	0.42	1.716
Ag/Ag′	177.41	61.20	−510 448.22	277.89	0.33	0	2.033
Gg′/G′g	65.20	−66.60	−510 447.33	277.89	1.22	0.89	1.993

around the CH_2-CH_2 bond. Later on, a conformational study was undertaken by microwave spectroscopy.[28] In that microwave study, it was claimed that four different conformers contribute to the observed spectra (see Figure 1), with the Gg conformer being the most populated form [Gg (33%), Ga (30%), Ag (28%), and Aa (9%) at 233 K]. Molecular mechanics and STO-3G *ab initio* calculations yield the Aa conformer as the most stable form,[29−31] while *ab initio* calculations carried out at higher levels of theory yield Ga or Gg as the conformational ground state, depending on the basis set and method used.[31] All calculations agree that the energy differences between the different conformers of *n*-propanol are very small (less than 3 kJ mol^{-1}). The uncertainty in the experimental results may also be appreciable, because the intensities of transitions in microwave experiments are proportional to the square of the molecular dipole moment and the three conformers proposed as being the most populated forms in the microwave study have dipole moments ranging from 1.72 to 2.03 D [DFT/B3LYP/6-311++G(d,p) results obtained in the present study], whereas the Aa conformer has the lowest dipole moment (1.65 D). Hence, Aa represents the most difficult species to be detected in the microwave spectra, and its relative population might have been underestimated in the experimental study. Analogous situations have been reported for glycine and glycolic acid.[32,33]

An infrared matrix-isolation study of *n*-propanol has already been reported.[31] Evidence was found of the presence of at least two conformers differing in the orientation of the C−C−C−O axis, although these were not clearly identified. Indeed, the matrix-isolation study failed in obtaining well-isolated monomers of *n*-propanol, with the spectra revealing extensive aggregation of the compound, which precluded any unambiguous analysis of the data for the monomers.

In the present study, we started by performing a series of systematic structural and vibrational calculations on monomeric *n*-propanol, to obtain a suitable characterization of the vibrational signature of its different possible conformers. The DFT/B3LYP method with the 6-311++G(d,p) basis set has already been used successfully in our laboratories to study several systems exhibiting conformers of nearly equal energy and low barriers to internal rotation[21,34,35] and was selected for the calculations.

Figure 1 and Table 1 present the structures of the five conformers of *n*-propanol, determined by DFT/B3LYP/6-311++G(d,p) calculations, and the relevant dihedral angles, total and relative energies, zero-point energies (ZPEs), and dipole moments for all of these forms. In agreement with previous theoretical data,[29−31] the calculations predict the Aa conformer as the most stable form, with an energy that is only slightly smaller (by less than 2 kJ mol^{-1}) than those calculated for the remaining forms. Note that Aa becomes the lowest energy conformer only when ZPE is taken into consideration (see Table 1), because of its relatively smaller ZPE. Using the calculated relative energies (with ZPE correction) and assuming the Boltzmann distribution, the populations for the five conformers at room temperature (300 K) were estimated as Aa/Ga/Ag/Gg/Gg′ = 14:27:24:20:16; i.e., all conformers should be present in the equilibrium in significant amounts. At 233 K, the predicted relative populations are 14:28:24:19:15, thus being in relatively good agreement with the values reported experimentally 9:30:28:33. Gg′ was not identified in the microwave study;[28] interestingly, the putative population for Gg reported in the microwave study is nearly equal to the sum of the calculated populations for Gg and Gg′ conformers in the present study. For the deuterated molecule, in a given enantiomer, G′g′, G′g, G′a, and Ag′ are no longer spectroscopically equivalent to Gg, Gg′, Ga′, and Ag. Their ZPEs are different (Table 2), and then, all 9 possible conformers need to be considered as different species. Indeed, each group of four conformers is equivalent to the other group in the other enantiomer, which, on the whole, makes the two enantiomers spectroscopically equivalent. The estimated populations at 300 K are, for (*R*)-*n*-[1-D]propanol, Aa/Ga/G′a/Ag/Ag′/Gg/G′g′/Gg′/G′g = 7:14:14:11:11:12:13:9:9 (i.e., when the populations of each pair of conformers that are energetically and spectroscopically equivalent in the nonsubstituted species are summed, the populations are nearly the same in *n*-propanol and *n*-propanol-1D).

TABLE 2: Zero-Point Energy (ZPE) and Zero-Point-Corrected Relative Energy (ΔE_{ZPE}) for the different conformers of (*R*)-*n*-[1-D]Propanol and (*S*)-*n*-[1-D]Propanol, Calculated at the DFT/B3LYP/6-311++G(d,p) Level of Theory

	(*R*)-*n*-[1-D]propanol		(*S*)-*n*-[1-D]propanol	
conformer	ZPE (kJ mol^{-1})	ΔE_{ZPE} (kJ mol^{-1})	ZPE (kJ mol^{-1})	ΔE_{ZPE} (kJ mol^{-1})
Aa	274.93	0.01	274.93	0.01
Ga	275.00	0	275.03	0.03
G′a	275.03	0.03	275.00	0
Gg	275.41	0.76	275.29	0.64
G′g′	275.29	0.64	275.41	0.76
Ag	275.42	0.35	275.27	0.2
Ag′	275.27	0.2	275.42	0.35
Gg′	275.22	1.04	275.42	1.24
G′g	275.42	1.24	275.22	1.04

Table 3 shows the DFT/B3LYP/6-311++G(d,p) calculated vibrational frequencies and calculated intensities (both in infrared and in Raman) corresponding to the ν_{O-H} and ν_{C-H} stretching modes in the five conformers of *n*-propanol and both (*R*)- and (*S*)-*n*-[1-D]propanol and to the $\nu_{C_\alpha-D}$ stretching vibration in the two deuterated isotopologues. From this table, it can be easily concluded that in the case of ν_{O-H}, as expected because of the essentially localized nature of the vibration, both the isotopic labeling and conformation around the C−C−C−O angle do not lead to any relevant changes in the frequency or intensities. These spectral parameters are, however, dependent on the value of the C−C−O−H dihedral angle, with the C−C−O−H anti conformers (Ga, G′a, and Aa) predicted to give rise to a higher frequency and more intense (both in IR and Raman) feature than the gauche conformers (Gg, G′g′, Ag, and Ag′). The Gg′ and G′g conformers show different spectral parameters for these two vibrations, which can be explained considering the existence in these conformers of the relatively more important interaction between the closely located OH and methyl

TABLE 3: Wavenumbers [$\tilde{\nu}$ (cm^{-1})] and Respective IR Intensities [I_{IR} (km mol^{-1})] and Raman Activities [A_R (Å^4 amu^{-1})] of the ν_{O-H}, $\nu_{C_\alpha-H}$ and $\nu_{C_\alpha-D}$ Vibrations of the Five Conformers of *n*-Propanol and (*R*)- and (*S*)-*n*-[1-D]Propanol Calculated at the DFT/B3LYP/6-311++G(d,p) Level of Theory[a]

	dihedral angles (X = H or D)				vibrational wavenumbers and intensities				
						ν_{C-H} (I_{IR}; A_R)			
conformer[b]	X_9COH (deg)	$X_{10}COH$ (deg)	X_9CCC (deg)	$X_{10}CCC$ (deg)	ν_{O-H} (I_{IR}; A_R)	ν_{C-H_2} as.	ν_{C-H_2} s.	$\nu_{C_\alpha-H}$	$\nu_{C_\alpha-D}$ (I_{IR}; A_R)
Gg	−59.53 (gauche′)	−175.13 (anti)	−174.40 (anti)	−56.02 (gauche′)					
n-propanol	H	H	H	H	3651 (23; 73)	3004 (29; 58)	2922[c,d] (39; 68)		
(*R*)-*n*-[1-D]propanol	D	H	D	H	3651 (23; 73)			3001 (32; 76)	2153 (43; 70)
(*S*)-*n*-[1-D]propanol	H	D	H	D	3651 (23; 75)			2924[e] (26; 77)	2205 (18; 52)
Ga	61.94 (gauche)	−57.30 (gauche′)	−175.67 (anti)	−57.04 (gauche′)					
n-propanol	H	H	H	H	3672 (32; 113)	2935 (33; 104)	2906 (64; 130)		
(*R*)-*n*-[1-D]propanol	D	H	D	H	3672 (32; 113)			2916 (52; 122)	2152 (42; 68)
(*S*)-*n*-[1-D]propanol	H	D	H	D	3672 (32; 113)			2927 (50; 95)	2142 (40; 58)
Ag	−62.80 (gauche′)	−178.33 (anti)	−58.39 (gauche′)	59.80 (gauche)					
n-propanol	H	H	H	H	3653 (23; 75)	3018[f] (83; 43)	2913[d] (58; 116)		
(*R*)-*n*-[1-D]propanol	D	H	D	H	3653 (22; 75)			3002 (17; 53)	2143 (39; 57)
(*S*)-*n*-[1-D]propanol	H	D	H	D	3653 (23; 76)			2917 (55; 105)	2207 (17; 51)
Aa	59.57 (gauche)	−59.57 (gauche′)	−59.21 (gauche′)	59.21 (gauche)					
n-propanol	H	H	H	H	3668 (29; 126)	2928 (44; 104)	2903 (62; 127)		
(*R*)-*n*-[1-D]propanol	D	H	D	H	3668 (29; 126)			2916 (52; 112)	2143 (39; 55)
(*S*)-*n*-[1-D]propanol	H	D	H	D	3668 (29; 126)			2916 (51; 112)	2143 (39; 55)
Gg′	173.04 (anti)	57.46 (gauche)	−177.24 (anti)	−59.00 (gauche′)					
n-propanol	H	H	H	H	3651 (22; 56)	3015[d] (38; 92)	2912[g] (57; 127)		
(*R*)-*n*-[1-D]propanol	D	H	D	H	3651 (22; 57)			2916 (54; 122)	2215 (20; 59)
(*S*)-*n*-[1-D]propanol	H	D	H	D	3651 (22; 56)			3012 (34; 116)	2142 (41; 60)

[a] Wavenumbers are scaled values, as described in the Experimental and Computational Methods. [b] Because of the symmetry equivalence of their geometries, the following pairs of conformers have equal vibrational signatures. In each indicated pair, the first conformer belongs to the *R* enantiomer and the second belongs to the *S* enantiomer: (Ga, G′a), (G′a, Ga), (Gg, G′g′), (G′g′, Gg), (Gg′, G′g), (G′g, Gg′), (Ag, Ag′), and (Ag′, Ag). [c] Out-of-phase with $C_\beta H_2$ s.; $\nu_{C_\alpha-H_2}$ s. in-phase with $C_\beta H_2$ s. is predicted to appear at 2935 cm^{-1} (I_{IR} = 57; A_R = 222). [d] In this vibration, the contribution of H_9 is larger than that of H_{10}. [e] Out-of-phase with $C_\beta H_2$ s.; $\nu_{C_\alpha-H_2}$ s. in-phase with $C_\beta H_2$ s. is predicted to appear at 2940 cm^{-1} (I_{IR} = 80; A_R = 186). [f] In-phase with $C_\beta H_2$ as. [g] In this vibration, the contribution of H_{10} is larger than that of H_9.

groups (see Figure 1). This interaction leads to unique perturbations in both geometric and electronic properties of the molecule (for example, this repulsion is also clearly reflected in the larger C−C−O−H and C−C−C−O dihedral angles predicted for Gg′ and G′g; see Table 1), which reflect themselves in the peculiar spectroscopic properties of these conformers.

In the case of the $\nu_{C_\alpha-H}$ stretching vibrations, the vibrational coupling between the two C_α−H bonds in the nondeuterated molecule leads to the presence of symmetric and antisymmetric modes. The usual repulsion of the energy levels associated with this extensive coupling implies that, for all conformers, the symmetric mode has a lower frequency, while the antisymmetric mode occurs at a higher frequency than that corresponding to the vibration of the isolated C_α−H bond in both (*R*)- and (*S*)-*n*-[1-D]propanol. Interestingly, with very few exceptions, the symmetric mode has systematically higher IR and Raman intensities than the vibration associated with the single C_α−H bond in the deuterated species, whereas the antisymmetric mode has, in general, lower intensities than these latter species (see Table 3). The spectral parameters associated with the $\nu_{C_\alpha-H}$ vibrations were also found to depend considerably on the molecular conformation. As it will be shown below, they are determined mainly by the values of the H−C−O−H and H−C_α−C−C dihedrals. In the nondeuterated molecule, the existence of two hydrogen atoms in the α carbon makes the analysis in terms of individual H−C−O−H and H−C_α−C−C dihedral angles very complex. However, a simple trend, resulting from averaging of the effects associated with the four H−C−O−H and H−C_α−C−C dihedral angles (two per each α-hydrogen atom), can be correlated with the C−C−O−H angle: both $\nu_{C_\alpha-H}$ symmetric and antisymmetric vibrations have higher frequencies in the conformers with a gauche C−C−O−H axis.

Interestingly, this is the opposite trend followed by the ν_{O-H} mode.

For the deuterated compounds, the dependence of the spectral parameters associated with the individual $\nu_{C_\alpha-H}$ vibration with the H−C−O−H and H−C_α−C−C dihedral angles can be clearly stated. Moreover, the predicted trends for the dependence of the spectral parameters of the $\nu_{C_\alpha-D}$ vibration with the D−C−O−H and D−C_α−C−C were found to be similar. The frequency of the $\nu_{C_\alpha-H/D}$ modes were found to decrease with the number of gauche arrangements, with a gauche D−C−O−H angle leading to a more pronounced effect of ∼60 cm^{-1} than a gauche D−C_α−C−C angle, which resulted in an effect of ∼10 cm^{-1}, {e.g., for (*R*)-*n*-[1-D]propanol, the number of gauche (D−C−O−H and D−C_α−C−C) arrangements for the Gg′, Ag′, G′g′, Gg, Ga, Ag, Aa, G′a, and G′g forms are (0,0), (1,0), (1,0), (0,1), (0,1), (1,1), (1,1), (1,1), and (1,1), respectively, and the corresponding $\nu_{C_\alpha-D}$ predicted frequencies are 2215, 2207, 2205, 2153, 2152, 2143, 2143, 2142, and 2142 cm^{-1}; see Table 3}. The IR intensities are mostly dependent on the H/D−C−O−H dihedral, being higher for a gauche conformation of this angle. On the other hand, the two angles (H/D−C−O−H and H/D−C_α−C−O) are relevant in determining the Raman activities, once again with gauche conformations giving rise to the most intense bands.

Once the pattern of variation of the relevant spectral parameters with the molecular conformation has been established theoretically, it is now possible to examine the experimental spectra of *n*-propanol and (*R*,*S*)-*n*-[1-D]propanol isolated in an inert matrix at low temperature. Under the experimental conditions used, the spectra are dominated by features because of monomeric species, with minor bands because of aggregates being easily identified on the basis of matrix concentration experiments.

Figure 2 shows the spectra of matrix-isolated *n*-propanol in the ν_{O-H} region and (*R*,*S*)-*n*-[1-D]propanol in both the ν_{O-H} and $\nu_{C_\alpha-D}$ stretching regions (the complexity of the ν_{C-H} region in the spectra of both molecules, because of methyl and ν_{C_b-H} methylenic vibrations, precludes any detailed analysis of this region. It would, however, be interesting to look at this region in the spectra of CD_3CD_2CDHOH). The splitting observed in both ν_{O-H} and $\nu_{C_\alpha-D}$ spectral regions demonstrates the contribution to the spectra of several conformers, as expected.

The ν_{O-H} region of both light and isotopically substituted compounds is identical and shows five overlapping peaks at 3665, 3662, 3660, 3658, and 3657 cm^{-1}, here tentatively assigned to Ga, Aa, Gg′, Ag, and Gg, respectively, on the basis of the calculated frequencies. Results of band deconvolution of this spectral region are presented in Figure 3. From the relative intensities of the component bands, weighted by the corresponding calculated intensities (see Table 3), the populations of the different conformers existing in the gaseous phase immediately prior to deposition of the matrix ($T = 300$ K) could be estimated as Aa/Ga/Ag/Gg/Gg′ = 7:29:25:25:14, which compares well with those obtained theoretically (14:27:24:20:16).

The $\nu_{C_\alpha-D}$ region of the deuterated compound shows a complex profile within the spectral range of 2204−2120 cm^{-1}. Taking into consideration the theoretical results, we could expect two main groups of bands: the first group, at lower frequencies (∼2168−2120 cm^{-1}), originating from all $\nu_{C_\alpha-D}$ single bonds showing a gauche (or gauche′) orientation regarding the D−C_α−O−H dihedral angle and corresponding to six different conformers of each enantiomer of *n*-[1-D]propanol (Aa, Ga, and G′a of both enantiomers, Gg, Ag, and G′g of (*R*)-*n*-[1-D]-propanol, and G′g′, Ag′, and Gg′ conformers of (*S*)-*n*-[1-D]-propanol); and the second considerably less intense group, at higher frequencies (∼2204−2168 cm^{-1}), associated with $\nu_{C_\alpha-D}$ single bonds anti to the O−H bond appearing in the Gg′, G′g′, and Ag′ conformers of (*R*)-*n*-[1-D]propanol as well as in the G′g, Gg, and Ag forms of (*S*)-*n*-propanol (see also Table 3). The dispersion in both of these groups is attributed to the presence of both gauche and anti conformations about the D−C_α−C−C torsion angle.

It is interesting to note that in consonance with the theoretical results and the proposed assignments, in the mixed (*R*,*S*)-*n*-[1-D]propanol sample the three conformers with the C−C−O−H axis in the anti conformation (Ga, G′a, and Aa) contribute only to the total intensity of the lower frequency $\nu_{C_\alpha-D}$ region, while

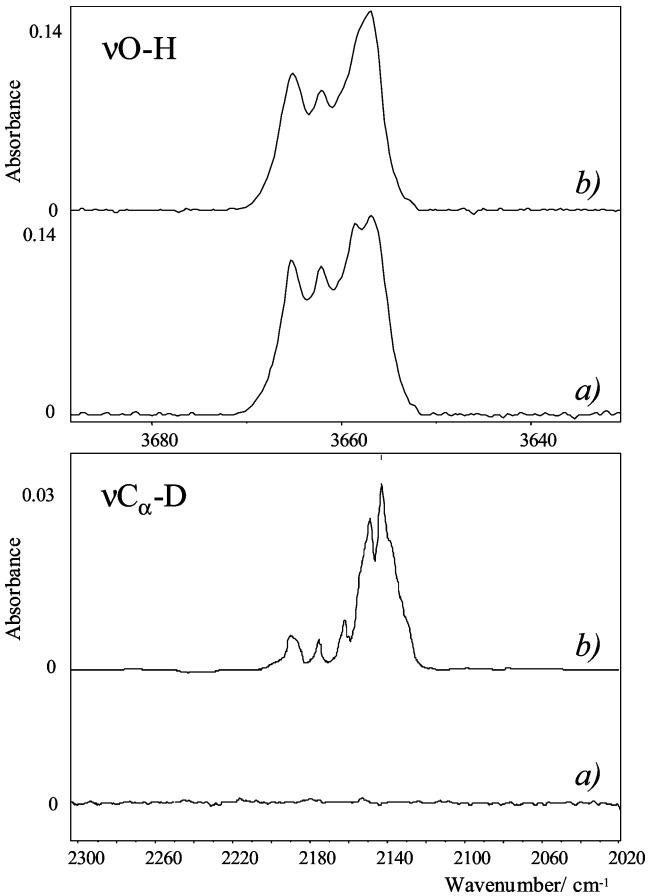

Figure 2. Infrared spectra of *n*-propanol (a) and (*R*,*S*)-*n*-[1-D]propanol (b) isolated in an argon matrix ($T = 8$ K; temperature of the nozzle, 300 K) in the ν_{O-H} and $\nu_{C_\alpha-D}$ stretching regions.

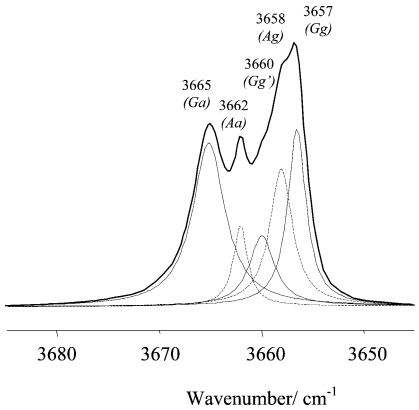

Figure 3. Deconvolution of the ν_{O-H} stretching region of the infrared spectum of matrix-isolated *n*-propanol.

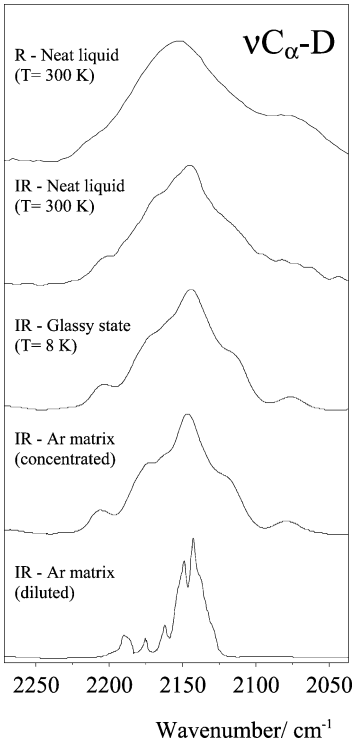

Figure 4. Infrared (IR) and Raman (R) $\nu_{C_\alpha-D}$ stretching region of the spectra of (*R*,*S*)-*n*-[1-D]propanol isolated in diluted and concentrated argon matrixes and in the neat glassy and liquid states.

those with a gauche (or gauche′) C−C−O−H axis contribute to the total intensity in both higher and lower frequency regions. If we consider the theoretically predicted intensities for these latter forms contributing to each one of the two spectral regions (see Table 3), taking into consideration their relative populations predicted by the calculations, it can be estimated that their contribution to the lower frequency region shall be approximately twice that to the higher frequency region. Considering also the intensity contributions from the remaining conformers to the lower frequency region (again taking into consideration the calculated intensities and relative populations), the intensity ratio between the lower and higher frequency $\nu_{C_\alpha-D}$ region in the matrix-isolation infrared spectrum of (*R*,*S*)-*n*-[1-D]propanol can be estimated as 5.0, which fits nicely to the observed integrated intensity ratio (5.5 ± 1).

Hydrogen-Bonding Studies. *Concentrated Matrixes, Neat Liquid, and Frozen Glass.* In concentrated matrixes, ν_{O-H} for small aggregates of *n*-propanol and (*R*,*S*)-*n*-[1-D]propanol appears at 3525 cm^{-1}, while higher order aggregates give rise to a very broad infrared band with main maxima at 3366 and 3278 cm^{-1}. In the neat liquid (room temperature; both IR and Raman), the bands because of ν_{O-H} originated in aggregates of different size overlap extensively and a single asymmetric broad band with maximum at ca. 3340 cm^{-1} is observed. In the $\nu_{C_\alpha-D}$ stretching region (Figure 4), aggregation leads essentially to band broadening and extension of the absorption range in both sides of the absorptions because of the monomeric species: the set of features associated with $\nu_{C_\alpha-D}$ in concentrated matrixes (with an estimated amount of monomer less than 5%) extend from ca. 2230 to 2060 cm^{-1}, with a global maximum at 2147 cm^{-1}. Interestingly, the frequency of the global maximum in the $\nu_{C_\alpha-D}$ stretching region was found to be similar in concentrated and diluted matrixes. This result clearly indicates that when the OH group is *simultaneously* acting as a hydrogen-bond donor and hydrogen-bond acceptor no correlation can be established between hydrogen-bond formation and the frequency

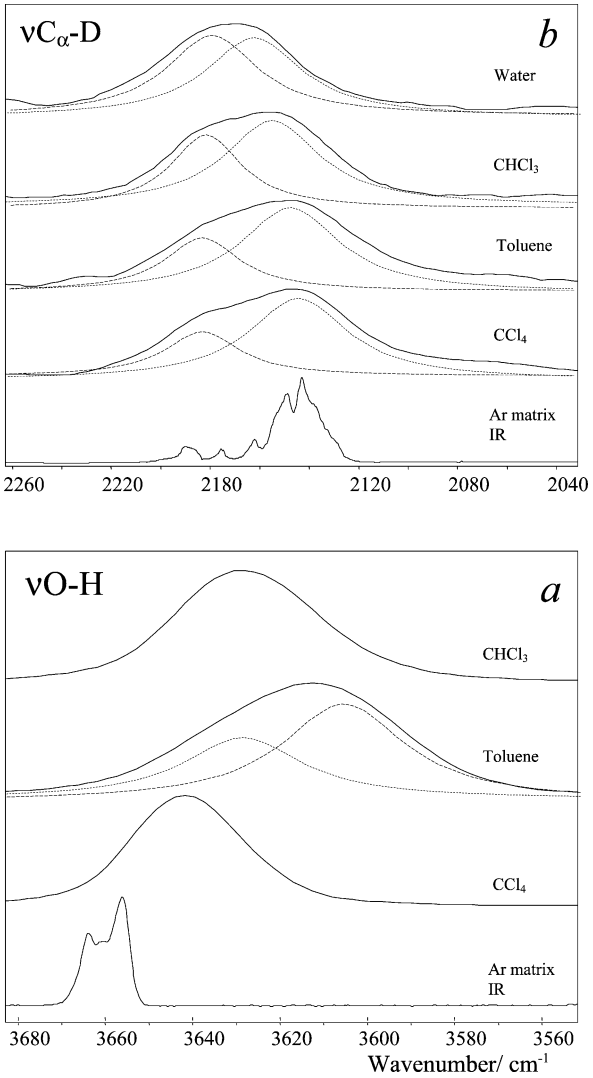

Figure 5. Raman spectra of (*R*,*S*)-*n*-[1-D]propanol solutions (10 mM; $T = 300$ K) in different solvents and infrared spectrum of the matrix-isolated compound (diluted matrix; $T = 8$ K; temperature of the nozzle, 300 K) in the ν_{O-H} and $\nu_{C_\alpha-D}$ stretching regions. Band deconvolution results are also shown in the figure (- - -).

of the $\nu_{C_\alpha-D}$ stretching vibration. This result is reinforced by the analysis of the spectra of the neat liquid compound and glassy state (IR spectrum obtained after fast deposition of the room temperature vapor of the compound on the CsI support of the cryostat kept at 8 K), where the $C_\alpha-D$ stretching region shows a profile similar to that found for the concentrated matrixes.

Solution (Solvents of Different Polarity). The Raman spectra of (*R*,*S*)-*n*-[1-D]propanol in dilute (10 mM) solutions of different solvents were also obtained (Figure 5), to inspect the influence of the polarity of the media on the vibrational frequencies. Aprotic solvents with different polarities were selected: chloroform ($\mu = 1.86$ D; $\epsilon/\epsilon_0 = 4.80$), toluene ($\mu = 0.38$ D; $\epsilon/\epsilon_0 = 2.40$), and carbon tetrachloride ($\mu = 0.00$ D; $\epsilon/\epsilon_0 = 2.20$).

In the ν_{O-H} spectral region of the spectra obtained in both carbon tetrachloride and chloroform, a single band is observed at 3643 and 3630 cm^{-1}, respectively, as expected being red-shifted relative to those obtained for the compound isolated in argon and exhibiting a larger red shift in the more polar solvent. These trends are nicely fitted by the PCM calculations presented in Table 4, and then, these bands are easily assigned to free (*R*,*S*)-*n*-[1-D]propanol monomers. In the case of the spectrum obtained for the compound in toluene, two overlapping bands

TABLE 4: Experimental and Calculated PCM/DFT/B3LYP/6-311++G(d,p) ν_{O-H} and $\nu_{C_\alpha-D}$ Frequencies of (*R*,*S*)-*n*-[1-D]Propanol in CCl_4, $CHCl_3$, and H_2O

	ν_{O-H}[a] (cm^{-1})				$\nu_{C_\alpha-D}$[a,b] (cm^{-1})							
					R				*S*			
conformer	isolated molecule	CCl_4	$CHCl_3$	H_2O	isolated molecule	CCl_4	$CHCl_3$	H_2O	isolated molecule	CCl_4	$CHCl_3$	H_2O
Ga	3672	3651	3632	3446	2152	2156	2158	2153	2142	2146	2148	2156
Aa	3668	3650	3631	3445	2143	2148	2151	2153	2143	2148	2151	2152
Gg′	3665	3749	3641	3394	**2215**	**2214**	**2212**	**2193**	2142	2148	2153	2166
Ag	3653	3633	3610	3358	2143	2147	2150	2152	**2207**	**2205**	**2204**	**2187**
Gg	3651	3634	3615	3429	2153	2158	2160	2160	**2205**	**2204**	**2203**	**2192**
observed	3660	3643	3630	*c*	**2176**	**2185**	**2183**	**2177**	**2176**	**2185**	**2183**	**2177**
					2146	2146	2151	2166	2146	2146	2151	2166

[a] Calculated vibrational frequencies are scaled as described in the Experimental and Computational Methods. [b] The assignment of the high-frequency experimental $\nu_{C_\alpha-D}$ bands to individual conformers is indicated by bolding the corresponding calculated frequencies. In all cases, conformers with an anti $D-C_\alpha-O-H$ axis are shown to give rise to these bands (see also Table 3). [c] Very broad band.

appear in this spectral region. Band deconvolution yields band maxima of the component bands at 3627 and 3606 cm^{-1}. The higher frequency component appears at a frequency close to that observed for chloroform and is due to essentially non-hydrogen-bonded *n*-[1-D]propanol monomers, while the lower frequency component is, with all probability, due to the hydrogen-bonded π complex of *n*-[1-D]propanol with toluene.

In the $\nu_{C_\alpha-D}$ region, the Raman spectrum of *R*,*S*-*n*-[1-D]-propanol obtained in solution, as for the matrix-isolated compound, exhibits two main features centered around 2150 and 2180 cm^{-1}, whose assignment is the same here proposed for the spectra of the compound in argon; i.e., the three conformers with the C−C−O−H axis in the anti conformation (Ga, G′a, and Aa) contribute only to the total intensity of the lower frequency $\nu_{C_\alpha-D}$ region, while those with a gauche (or gauche′) C−C−O−H axis (the remaining six conformers) contribute to the total intensity in both higher and lower frequency regions with 1:2 approximate relative contributions. In this spectral region, the PCM calculations indicate that the bands appearing in the lower frequency region shall increase with the polarity of the media, whereas those appearing in the higher frequency region shall decrease. Accordingly, the observed frequencies in carbon tetrachloride, toluene, and chloroform are 2185, 2183, and 2183 cm^{-1} and 2146, 2146, and 2151 cm^{-1}. Very interestingly, these trends were also followed when going to a water (μ = 2.95 D; ϵ/ϵ_0 = 78.4)[37] solution (see Figure 5b), with the higher and lower frequency component bands appearing at 2177 and 2166 cm^{-1}, respectively, thus being also in consonance with the PCM predictions.

On the whole, these results demonstrate that the solvent plays a significant role in determining the frequency of both the ν_{O-H} and $\nu_{C_\alpha-D}$ stretching modes. Hence, any attempt to correlate the hydrogen-bond strengths with the vibrational frequencies should be restricted to studies performed in the same solvent or, at least, should require that a calibration procedure be applied to compare data obtained in different solvents. In particular, studies should be undertaken in solvents that do not have a propensity for even weak hydrogen-bonding interactions.

It is also interesting to look at the relative intensities of the two features (around 2150 and 2180 cm^{-1}) appearing in the $\nu_{C_\alpha-D}$ stretching region. The results shown in Figure 5b clearly indicate that the intensity of the band at 2180 cm^{-1} increases considerably, compared to that of the band at 2150 cm^{-1}, with the polarity of the solvent, thus indicating that the amount of C−C−O−H gauche conformers increases in more polar solvents (as discussed above, only conformers with a gauche C−C−O−H axis contribute to the feature at ca. 2180 cm^{-1}, while all conformers contribute to the feature at ca. 2150 cm^{-1}, with the contribution of the three C−C−O−H anti conformers, Ga, G′a, and Aa, to this latter band being dominant). The stabilization of the C−C−O−H gauche conformers in more polar media is in agreement with their larger dipole moments (strictly this is true only for Ag/Ag′ and Gg′/G′g, which have dipole moments of ca. 2 D. the Gg/G′g′ conformers have a dipole moment, 1.71 D, that does not differ very much from those of the Aa and Ga/G′a forms, which are 1.65 and 1.78 D, respectively; however, at room temperature, Ag/Ag′ and Gg′/G′g constitute ca. 67% of the population of C−C−O−H gauche conformers).

SCHEME 1: Triethylamine, *N*,*N*-Diisopropylethylamine, *N*-Methylmorpholine, and *N*,*N*-Dimethylaniline

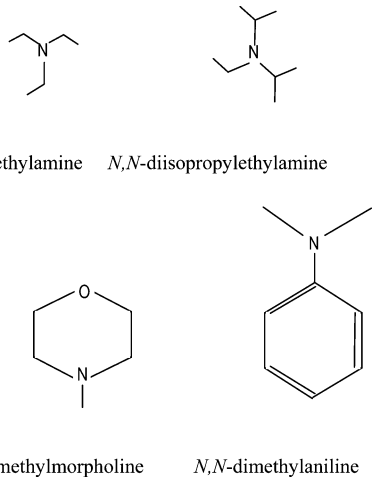

Mixed ($CHCl_3$) Solutions of (R,S)-n-[1-D]Propanol and Tertiary Amines. In the previous sections, we concluded that using a fixed solvent is a required condition to allow us to extract information on the hydrogen-bonding strengths from the frequency of the $\nu_{C_\alpha-D}$ stretching region. In addition, it was concluded that it is also required that the hydrogen-bond donor species is not simultaneously participating in hydrogen bonding as an acceptor. Hence, in this section, we look at the hydrogen-bonding processes involving the interaction between (*R*,*S*)-*n*-[1-D]propanol and tertiary amines in chloroform solution [tertiary amines are expected to act only as hydrogen-bond acceptors, because they do not have any hydrogen atoms bounded to the nitrogen atom; the possible very weak C−H (amine)···O (propanol) hydrogen bonds are not expected to play any relevant role here, because they shall not be distinguishable from those involving the solvent]. A series of tertiary amines with different pK_a values was selected (Scheme 1): triethylamine (pK_a = 11.2), *N*,*N*-diisopropyl-ethylamine (pK_a = 11.0), *N*-methylmorpholine (pK_a = 7.7), and *N*,*N*-dimethylaniline (pK_a = 6.6). The trigonal pyramidal arrangement of bonds around the nitrogen atom is less pronounced in the arylamine here

TABLE 5: $\nu_{C_\alpha-D}$ Stretching Frequencies of (*R*,*S*)-*n*-[1-D]Propanol in $CHCl_3$ Mixed Solutions with Tertiary Amines of Different Basicities

$\nu_{C_\alpha-D}$ (cm^{-1})	$CHCl_3$	dimethylaniline pK_a = 6.6	methylmorpholine pK_a = 7.7	diisopropylethylamine pK_a = 11.0	triethylamine pK_a = 11.2
higher frequency band	2183	2165	2164[a], 2137[b]	2152	2150
lower frequency band	2151	2138	2137[a], 2114[b]	2128	2124

[a] $\nu_{C_\alpha-D}$ stretching of (*R*,*S*)-*n*-[1-D]propanol because of the intermolecular hydrogen bond O−$H_{al.}$···N. [b] $\nu_{C_\alpha-D}$ stretching of (*R*,*S*)-*n*-[1-D]propanol because of the intermolecular hydrogen bond O−$H_{al.}$···O.

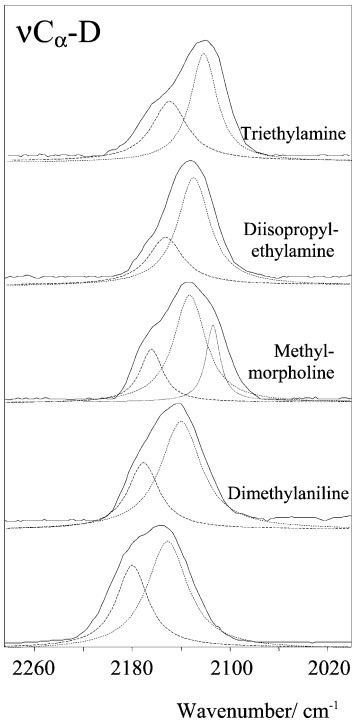

Figure 6. $\nu_{C_\alpha-D}$ stretching region of the Raman spectra of (*R*,*S*)-*n*-[1-D]propanol (10 mM)/tertiary amines (500 mM) mixed solutions (T = 300 K) in chloroform and Raman spectrum of (*R*,*S*)-*n*-propanol-1D (10 mM) in the same solvent. Band deconvolution results are also shown in the figure (- - -).

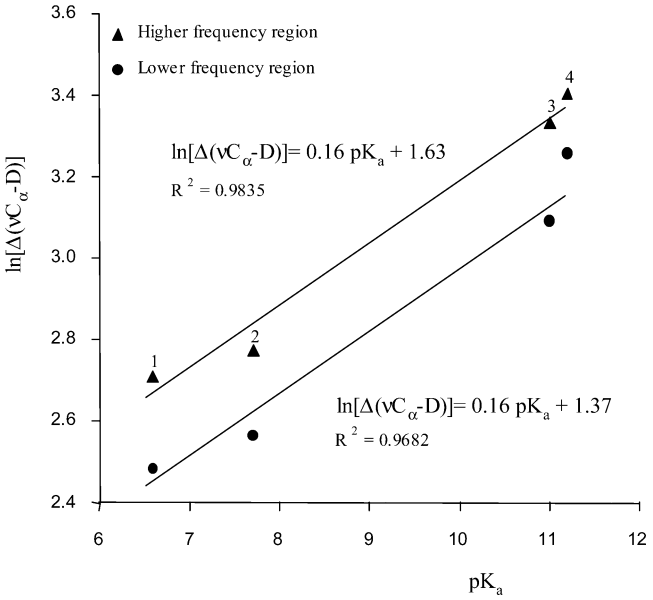

Figure 7. Plot of the frequency shift associated with the hydrogen-bond formation, $\Delta(\nu_{C_\alpha-D})$, as a function of the pK_a of the amines: (1) *N*,*N*-dimethylaniline, (2) *N*-methylmorpholine, (3) *N*,*N*-diisopropylethylamine, and (4) triethylamine.

considered (*N*,*N*-dimethylaniline) than in the alkylamines, as a result of the resonance delocalization of the nitrogen lone pair toward the aromatic π system; such delocalization is responsible for the decrease in the basicity of this compound relative to the remaining (alkyl) amines. While *N*-methylmorpholine has two potential hydrogen-bond acceptor centers, the O atom of the ring is estimated to have a pK_a value of at least 6 log units lower than N.

The Raman spectra obtained for the mixed ($CHCl_3$) solutions of (*R*,*S*)-*n*-[1-D]propanol and tertiary amines are shown in Figure 6. In all cases, the $\nu_{C_\alpha-D}$ stretching bands are red-shifted relative to their position in the spectrum of (*R*,*S*)-*n*-[1-D]propanol in $CHCl_3$, with the red shifts increasing with the basicity of the amine, i.e., with the strength of the hydrogen bond (Table 5). Note that the pattern revealed by deconvolution of the $\nu_{C_\alpha-D}$ bands in the spectrum of the mixed *n*-[1-D]propanol/*N*-methylmorpholine solution shows that the presence of the O results in a much stronger interaction, potentially through a bifurcated hydrogen bond.

Figure 7 shows a plot of the frequency shift associated with the hydrogen-bond formation, $\Delta(\nu_{C_\alpha-D})$, as a function of the pK_a of the amines. The experimental points fit well to a straight line, obeying the general equation $\ln[\Delta(\nu_{C_\alpha-D})] = 0.16pK_a + \zeta$, with ζ being a parameter that is characteristic of the particular feature under analysis (ζ = 1.63 and 1.37, for the higher and lower $\nu_{C_\alpha-D}$ component bands, respectively). The slopes for the two straight lines are not distinguishably different, indicating that the effect of changing the acceptor is felt similarly in both cases. On the other hand, the different intercepts indicate a different hydrogen-bonding ability of the donor conformations, which will be slightly better for the species giving rise to the higher frequency band. Indeed, as already mentioned, the higher frequency band is originated in the most polar gauche C−C−O−H conformers of (*R*,*S*)-*n*-[1-D]propanol, which are also those exhibiting a longer O−H bond length and lower ν_{O-H} stretching frequency (see also Table 3), thus giving full support to the experimental findings.

Conclusion

The correlation of $\nu_{C_\alpha-D}$ with the conformation and hydrogen-bonding interactions of a primary alcohol have provided a further basis for the interpretation of specifically deuterated alcohols when complexed at an enzyme active site. The D−C_α−O−H torsion angle has the greatest effect on $\nu_{C_\alpha-D}$, where an anti-lone pair reduces the observed frequency by ~60 cm^{-1} in calculations and by an observed 30−40 cm^{-1} experimentally. The D−C_α−C−C torsion angle has a smaller effect, with the $\nu_{C_\alpha-D}$ being reduced by 10 cm^{-1} when anti to a methylenic C−H bond rather than a C−C bond. If the alcohol functions as an hydrogen-bond donor, $\nu_{C_\alpha-D}$ is red-shifted by an amount that correlates with the hydrogen-bond strength, ranging from 15 to 30 cm^{-1} as the basicity of the acceptor increased by 4.6 pK_a units. These observations may be used in conjunction with a known crystal structure to provide two sources of information: whether there is heterogeneity in the conformation of the bound

alcohol, and in addition, when the conformation of the bound molecule is known, to infer the strength of hydrogen-bond interactions.

Acknowledgment. This work was supported by grants from the "Fundação para a Ciência e a Tecnologia", Lisbon (Research Projects POCTI/QUI/43366/2001 and POCTI/QUI/33495/2000 and Grant SFRH/BD/6696/2001), FEDER, and the NSF (MCB 0110610). Computational support was provided by the Ohio Supercomputer Center.

References and Notes

(1) Fersht, A. *Enzyme Structure and Mechanism*, 2nd ed.; Freeman and Company, W. H.; New York, 1985.

(2) Vrielink, A.; Sampson, N. *Curr. Opin. Struct. Biol.* **2003**, *13*, 709.

(3) Gerlt, J. A.; Kreevoy, M. M.; Cleland, W. W.; Frey, P. A. *Chem. Biol.* **1997**, *4*, 259.

(4) Wishart, D. S.; Sykes, B. D.; Richards, F. M. *J. Mol. Biol.* **1991**, *222*, 311.

(5) (a) Piaggio, P.; Tubino, R.; Dellepiane, C. *J. Mol. Struct.* **1983**, *96*, 277. (b) Krueger, P. J.; Jan, J.; Wieser, H. *J. Mol. Struct.* **1970**, *5*, 375.

(6) Purcell, K. F. S.; Brunk, S. D. *J. Am. Chem. Soc.* **1969**, *91*, 4019.

(7) Rozenberg, M.; Shoham, G.; Reva, I. D.; Fausto, R. *Spectrochim. Acta, Part A* **2003**, *59*, 3253.

(8) Tonge, P. J.; Fausto, R.; Carey, P. R. *J. Mol. Struct.* **1996**, *379*, 135.

(9) D'Alva Torres, G. S. F.; Pouchan, C.; Teixeira-Dias, J. J. C.; Fausto, R. *Spectrosc. Lett.* **1993**, *26*, 913.

(10) Gawlita, E.; Lantz, M.; Paneth, P.; Bell, A.; Tonge, P.; Anderson, V. E. *J. Am. Chem. Soc.* **2000**, *122*, 11660.

(11) Maiti, N. C.; Carey, P. R.; Anderson, V. E. *J. Phys. Chem. A* **2003**, *107*, 9910.

(12) Dong, J.; Dinakarpandian, D.; Carey, P. R. *Appl. Spectrosc.* **1998**, *52*, 1117.

(13) Galactic Industries, Inc.; Origin, Peak Fitting Model, version 7.0300; copyright 1991−2002; Microcal software, Inc.

(14) Reva, I. D.; Stepanian, S.; Adamowicz, L.; Fausto, R. *J. Phys. Chem. A* **2001**, *105*, 4773.

(15) Frisch, M. J.; Trucks, G. W.; Schlegel, H. B.; Scuseria, G. E.; Robb, M. A.; Cheeseman, J. R.; Zakrzewski, V. G., Jr.; Montgomery, J. A.; Stratmann, R. E.; Burant, J. C.; Dapprich, S.; Millam, J. M.; Daniels, A. D.; Kudin, K. N.; Strain, M. C.; Farkas, O.; Tomasi, J.; Barone, V.; Cossi, M.; Cammi, R.; Mennucci, B.; Pomelli, C.; Adamo, C.; Clifford, S.; Ochterski, J.; Petersson, G. A.; Ayala, P. Y.; Cui, Q.; Morokuma, K.; Malick, D. K.; Rabuck, A. D.; Raghavachari, K.; Foresman, J. B.; Cioslowski, J.; Ortiz, J. V.; Stefanov, B. B.; Liu, G.; Liashenko, A.; Piskorz, P.; Komaromi, I.; Gomperts, R.; Martin, R. L.; Fox, D. J.; Keith, T.; Al-Laham, M. A.; Peng, C. Y.; Nanayakkara, A.; Gonzalez, C.; Challacombe, M.; Gill, P. M. W.; Johnson, B.; Chen, W.; Wong, M. W.; Andres, J. L.; Head-Gordon, M.; Replogle, E. S.; Pople, J. A. *Gaussian 98*, revision A.3; Gaussian, Inc.: Pittsburgh, PA, 1998.

(16) McLean, A. D.; Chandler, G. S. *J. Chem. Phys.* **1980**, *72*, 5639.

(17) Clark, T.; Chandrasekhar, J.; Spitznagel, G. W.; Schleyer, P. V. R. *J. Comput. Chem.* **1983**, *4*, 294.

(18) Frisch, M. J.; Head-Gordon, M.; Pople, J. A. *Chem. Phys. Lett.* **1990**, *166*, 281.

(19) Becke, A. D. *J. Chem. Phys.* **1993**, *98*, 5648.

(20) Lee, C.; Yang, W.; Parr, R. G. *Phys. Rev.* **1988**, *B37*, 785.

(21) Gómez-Zavaglia, A.; Fausto, R. *Vib. Spectrosc.* **2003**, *33*, 105.

(22) Borba, A.; Gómez-Zavaglia, A.; Lapinski, L.; Fausto, R. *Phys. Chem. Chem. Phys.* **2004**, *6*, 2101.

(23) De Frees, D.; McLean, A. *J. Chem. Phys.* **1985**, *82*, 333.

(24) Miertus, S.; Scrocco, E.; Tomasi, J. *Chem. Phys.* **1981**, *55*, 117.

(25) Fukushima, K.; Zwolinski, B. *J. Mol. Spectrosc.* **1968**, *26*, 368.

(26) Plyler, E. K. *J. Res. Natl. Bur. St.* **1952**, *48A*, 281.

(27) Quinan, J. R.; Wiberley, S. E. *Anal. Chem.* **1954**, *26*, 1762.

(28) Abdurakhmanov, A. A.; Veliyulin, E. I.; Ragimova, R. A.; Imanov, L. M. *Zh. Strukt. Khim.* **1981**, *22*, 39.

(29) Mayer, A. Y. *J. Mol. Struct.* **1983**, *105*, 143.

(30) Teixeira-Dias, J. J. C.; Fausto, R. *J. Mol. Struct.* **1986**, *144*, 199.

(31) Lotta, T.; Murto, J.; Rasänen, M.; Aspiala, A. *Chem. Phys.* **1984**, *86*, 105.

(32) Suenram, R. D.; Lovas, F. J. *J. Mol. Spectrosc.* **1978**, *72*, 372.

(33) Reva, I. D.; Jarmelo, S.; Lapinski, L.; Fausto, R. *Chem. Phys. Lett.* **2004**, *389*, 68.

(34) Gómez-Zavaglia, A.; Fausto, R. *Phys. Chem. Chem. Phys.* **2003**, *5*, 52.

(35) Gómez-Zavaglia, A.; Fausto, R. *J. Mol. Struct.* **2004**, *689*, 199.

(36) Gubskaya, A. V.; Kusalik, P. G. *J. Chem. Phys.* **2002**, *117*, 5290.

(37) Wade, L. G. *Organic Chemistry*, 5th ed.; Prentice Hall Inc.: New York, 1995−2002; Chapter 21.